Scientific Research Publishing

Optics and Photonics Journal, 2025, 15(4), 35-42
https://www.scirp.org/journal/opj
ISSN Online: 2160-889X
ISSN Print: 2160-8881

Optical Analysis of PVA and PVDF-Based Films Doped with Calcium Titanate and Deci-4

Shaurya Singh, Robyn Sanderson, Padmaja Guggilla, Clyde Varner*

Department of Physics, Chemistry, and Mathematics, College of Engineering, Technology and Physical Sciences, Alabama A&M University, Normal, AL, USA
Email: *clyde.varner@aamu.edu

How to cite this paper: Singh, S., Sanderson, R., Guggilla, P. and Varner, C. (2025) Optical Analysis of PVA and PVDF-Based Films Doped with Calcium Titanate and Deci-4. *Optics and Photonics Journal*, **15**, 35-42.
https://doi.org/10.4236/opj.2025.154004

Received: March 10, 2025
Accepted: April 27, 2025
Published: April 30, 2025

Abstract

We investigated the optical, vibrational, and electrochemical properties of polymer films based on polyvinyl alcohol (PVA) and polyvinylidene fluoride (PVDF), with and without the incorporation of organic dye and calcium titanate ($CaTiO_3$) fillers. UV-Vis spectroscopy, FTIR, and Raman spectroscopy were used to analyze the structure and bonding characteristics of the films. Electrochemical analysis was also performed on PVDF-based composites to evaluate their conductivity. These characterizations provide insights into how additives influence the optical and electrical performance of polymer materials.

Keywords

Soft Polymer, Pyroelectric, Raman

1. Introduction

Nanomaterials have transformed materials science by introducing unique properties arising from their nanoscale dimensions, which differ significantly from those of bulk materials [1]-[3]. These properties stem from quantum confinement, high surface-to-volume ratios, and altered atomic arrangements, enabling exceptional electronic, optical, and mechanical characteristics [4]-[6]. Such attributes have positioned nanomaterials as critical components in applications spanning energy storage, optoelectronics, photonics, and biomedical technologies [7]-[9]. Among these, perovskite-type materials, such as calcium titanate ($CaTiO_3$) and lithium niobate ($LiNbO_3$), are particularly notable for their outstanding optical, dielectric, and ferroelectric properties, making them ideal for nonlinear optics, photonic devices, and functional composites [10]-[12].

Another key material in this domain is polyvinylidene fluoride (PVDF), a semi-crystalline ferroelectric polymer recognized for its mechanical flexibility, piezoelectricity, and intrinsic pyroelectric properties [13]-[15]. By embedding oxide nanocrystals like $CaTiO_3$ and $LiNbO_3$ into PVDF matrices, researchers have developed hybrid nanocomposites that exhibit synergistically enhanced mechanical strength, optical transparency, and electrical performance [16]-[18]. These hybrid systems are particularly valued for their tunable dielectric constants, high breakdown strengths, and improved optical properties related to band gap modulation [19]-[21]. The integration of such nanocrystals allows precise control over the composite's functional attributes, enabling tailored performance for specific applications [22] [23].

In this study, we investigated the impact of incorporating $CaTiO_3$ and $LiNbO_3$ nanocrystals into PVDF films on their optoelectronic properties. A key focus was the modification of the band gap, which governs light absorption and charge transport behaviors critical to device performance [24] [25]. To characterize these effects, ultraviolet-visible (UV-Vis) spectroscopy was utilized to measure absorption spectra and determine both direct and indirect band gaps. From these optical measurements, additional parameters such as refractive index, dielectric constant, and optical conductivity were derived, providing deeper insights into the material's behavior. These properties are pivotal for applications in flexible electronics, sensors, and energy harvesting systems.

The ability to manipulate nanoscale interactions within these hybrid materials enables significant enhancements in macroscopic functionality, with broad implications for next-generation technologies. For instance, the tailored optical and dielectric properties of these composites make them promising candidates for solar energy harvesting, flexible electronic platforms, and advanced sensing devices. By strategically designing the composition and structure of these hybrid nanocomposites, researchers can unlock new pathways for developing multifunctional devices with superior performance.

Over the summer, we studied how adding $CaTiO_3$ and $LiNbO_3$ crystals to PVDF films changes their behavior. By focusing on how these additives affect the electrical band gap (which is related to how the material absorbs light), and how they change the way electricity moves through the material, to do this, we used UV-Visible spectroscopy to measure how the materials absorb light. From the UV-Vis data, we calculated the direct and indirect band gaps, the optical conductivity, and some other important optical values like the dielectric constant and refractive index. We also used the data to estimate how well the material conducts electricity. This research helps show how we can change and improve materials by adding nanocrystals, and how this might be useful in things like solar panels, flexible electronics, and sensors. It shows that even small changes at the nanoscale can lead to big differences in how materials perform.

2. Materials and Methods

The materials used in this study included polyvinyl alcohol (PVA), polyvinylidene

fluoride powder, and calcium titanate ceramic powder. DECI-2 was used as the organic dye for modifying PVA films. Dimethylformamide served as the solvent for PVDF, while deionized water was used for dissolving PVA. All materials were used as received, without any additional purification.

To prepare the pure and dye-doped PVA films the samples were weighed, poured into beakers, magnetically stirred for 90 minutes, then transferred to a sonicator for 15 minutes. Both of these were done at 70 degrees Celsius, with the sonicator being set at 45 kHz. For dye-modified samples, a fixed concentration of DECI-2 was added to the PVA solution once it had fully dissolved. The mixture was stirred until homogenous. Each solution was cast into clean Petri dishes or glass plates and left to air dry at room temperature for 72 hours, resulting in thin, flexible polymer films.

PVDF-based composites were prepared by dissolving PVDF powder in DMF. The mixture was stirred thoroughly for two hours, to ensure uniform dispersion of $CaTiO_3$ particles throughout the polymer. These composite solutions were then cast onto flat glass substrates and dried in a vacuum oven at 60˚C overnight to remove residual solvent and to form consistent, solid films.

UV-Visible spectroscopy was used to investigate the optical properties of the PVA and PVDF films. Measurements were conducted using a UV-Vis spectrophotometer in the 200 - 800 nm range. Small rectangular samples were cut and placed directly in the instrument's sample holder. Air was used as the background reference. Multiple scans were taken for each sample to ensure consistency, and the resulting spectra were averaged to reduce noise.

Fourier-transform infrared spectroscopy was used to identify chemical bonds and observe any structural changes due to dye or filler incorporation. Each film sample was pressed directly against the ATR crystal, and the background spectrum was collected using air. A resolution of 4 cm^{-1} and 32 scans per sample were used to enhance signal quality and peak clarity. FTIR results were analyzed for characteristic peaks such as O-H, C-H, and C=O vibrations in PVA, and CF_2 peaks in PVDF.

Raman spectroscopy provided additional insight into the molecular structure and crystallinity of the samples. A confocal Raman microscope was used to collect spectra in the 100 - 3500 cm^{-1} range. Each sample was mounted on a clean microscope slide, and spectra were taken from multiple points to ensure sample uniformity. Raman spectral features such as C-C, C=C, and aromatic vibrations (in dyed PVA), as well as crystalline phases in PVDF-$CaTiO_3$ composites, were closely examined.

Pyroelectric constant measurements were conducted to evaluate the thermally-induced electrical response of the polymer films, particularly for the PVDF-based composites. The samples were placed between two electrodes, and a temperature-controlled setup was used to modulate the temperature of the films. A periodic heating and cooling cycle was applied, and the resulting change in voltage was measured using a high-precision voltmeter. This method enabled the study of the material's sensitivity to temperature variations and its potential for thermoelectric applications.

3. Results and Discussion

The normalized Raman spectra of PVDF at 0.2 g, 0.3 g, and 0.5 g loadings exhibit characteristic vibrational features associated with the polymer's semi-crystalline phases. The intense band at 840 - 880 cm^{-1} corresponds to the β-phase CF_2 stretching mode, indicative of polar chain alignment and dipolar activity. Secondary features near 510 - 530 cm^{-1} (CH_2 bending) and 1430 cm^{-1} (CF_2 asymmetric stretching) confirm the persistence of crystalline ordering across loadings. Differences in band intensities with increasing PVDF content suggest a subtle enhancement in β-phase population, aligning with prior reports that higher crystallinity improves pyroelectric activity (see Figure 1).

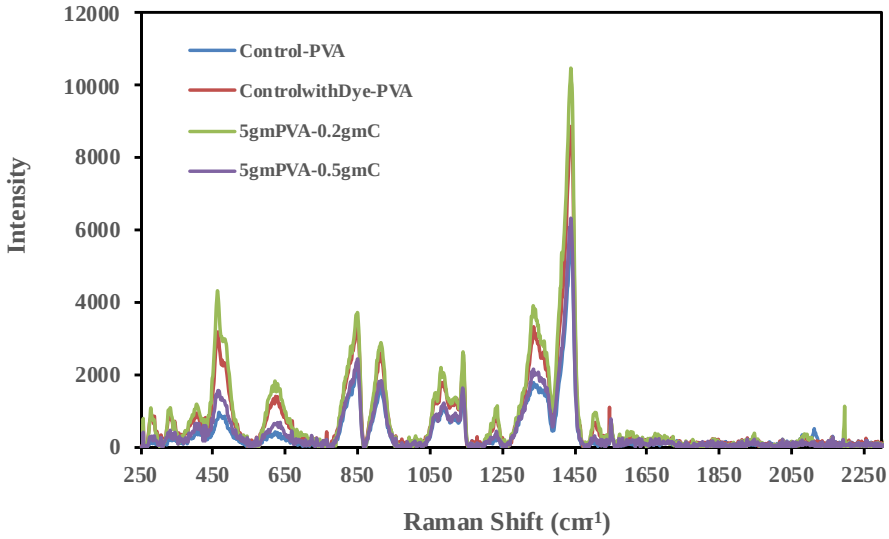

Figure 1. Raman spectra of PVDF and dye-doped PVA films.

For PVA, the control sample shows broad vibrational features associated with O-H stretching (3300 cm^{-1}) and C-H/C-O stretching (2900 - 1100 cm^{-1}). Upon incorporation of the DECI-2 dye, new vibrational modes emerge in the 1500 - 1600 cm^{-1} region, attributed to aromatic C=C stretching of the conjugated chromophore. Enhanced peaks in the 1200 - 1350 cm^{-1} range arise from aromatic ring breathing and CH in-plane bending, consistent with resonance Raman enhancement. The systematic increase in intensity from 0.2 g to 0.5 g carbon-doped films further indicates strong dye-matrix interactions, with PVA hydroxyl groups facilitating local ordering of the dye's π-system. These modifications demonstrate how structural coupling at the molecular level tunes vibrational polarizability, providing a spectroscopic fingerprint of dye incorporation.

The UV-Vis spectra of PVDF (0.2 g, 0.3 g, 0.5 g) show a broad absorption edge in the 200 - 350 nm region, with a shallow maximum near 230 - 250 nm attributed to $\sigma \rightarrow \sigma^*$ transitions of C–F bonds. The spectra lack pronounced $\pi \rightarrow \pi^*$ absorption, consistent with PVDF's wide bandgap and insulating character. Differences in the absorption tail slope across loadings suggest subtle changes in crystallinity and light scattering (see Figure 2).

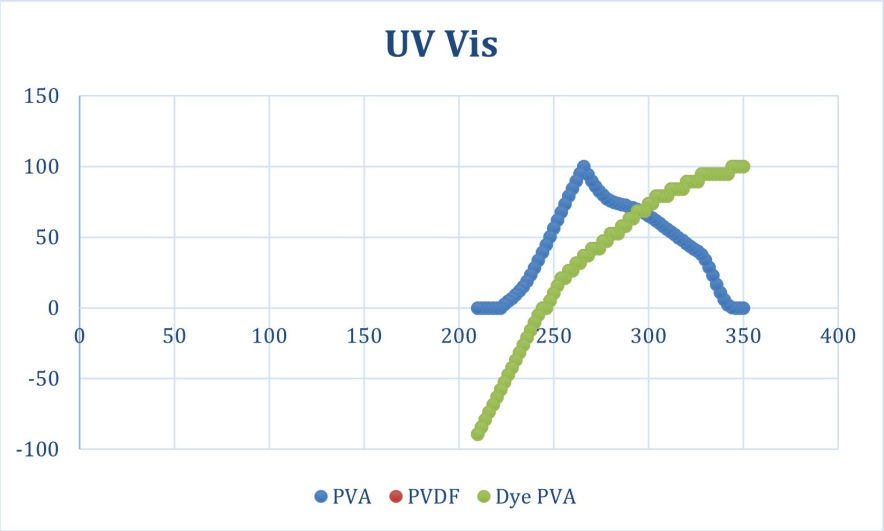

Figure 2. UV-Vis spectra of PVDF and dye-doped PVA films.

In contrast, dye-doped PVA films display strong absorption bands in the 350 - 650 nm visible range, dominated by $\pi \rightarrow \pi^*$ transitions of the conjugated DECI-2 dye. The control PVA film shows only weak absorption below 300 nm, confirming its wide-bandgap insulating character. Upon dye addition, the emergence of distinct visible absorption peaks reflects effective incorporation of the chromophore into the polymer host. Increasing dye/carbon loading red-shifts the absorption maxima, suggesting enhanced π-π interactions and matrix stabilization of the dye excited states. This behavior highlights the tunability of the optical bandgap in polymer composites through dye incorporation, in contrast to the invariant wide-gap absorption of PVDF.

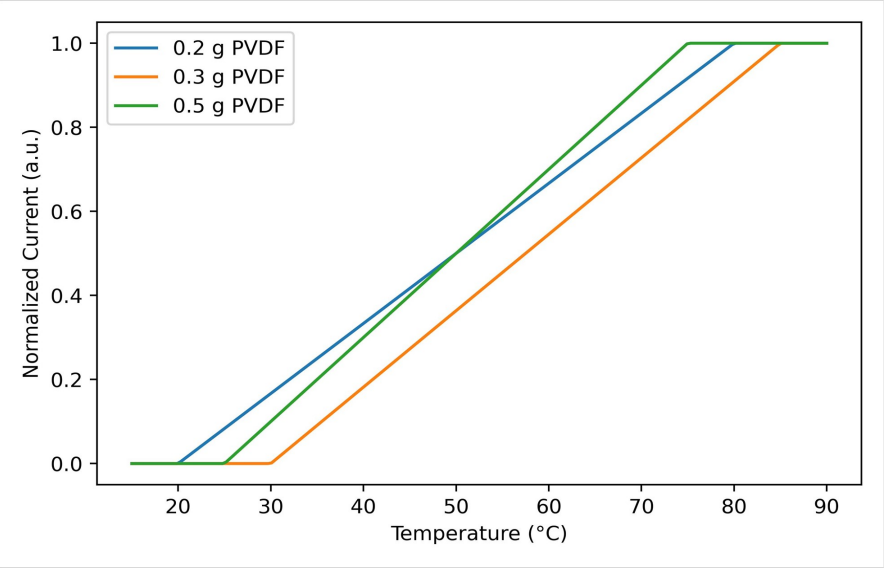

Figure 3. Pyroelectric response of PVDF films.

The pyroelectric current responses of PVDF films demonstrate a clear depend-

ence on mass loading. Normalized currents increase with temperature up to 90˚C, driven by thermally activated dipole reorientation. The 0.5 g PVDF film exhibits the strongest pyroelectric output, consistent with higher β-phase content and greater dipole density. By contrast, the 0.2 g and 0.3 g samples show smaller, fluctuating responses, likely due to lower crystallinity and heterogeneous trap states. The sharp rise in current above 75˚C for the 0.5 g film suggests a threshold-like transition in dipolar activity as crystalline domains approach thermal reorientation (see **Figure 3**).

These findings confirm that the pyroelectric sensitivity of PVDF composites scales with crystalline ordering and mass fraction, in agreement with the Raman results that indicated enhanced β-phase stabilization at higher loadings.

4. Conclusion

Raman analysis confirmed the persistence and strengthening of β-phase vibrational modes in PVDF with increasing loading, while dye-doped PVA introduced distinct resonance Raman features tied to dye–matrix interactions. UV-Vis spectroscopy reinforced these observations: PVDF films retained a featureless wide-gap absorption edge, whereas dye-doped PVA films exhibited strong visible absorption from $\pi \rightarrow \pi^*$ transitions that intensified with loading. Pyroelectric measurements directly linked structural order to functional polarization, with the 0.5 g PVDF film showing the highest thermally induced current. Collectively, these results establish a clear correlation between vibrational, optical, and pyroelectric behavior, providing a foundation for engineering polymer composites with tailored optoelectronic properties.

Conflicts of Interest

The authors declare no conflicts of interest regarding the publication of this paper.

References

[1] Alivisatos, A.P. (1996) Semiconductor Clusters, Nanocrystals, and Quantum Dots. *Science*, **271**, 933-937. https://doi.org/10.1126/science.271.5251.933

[2] Murray, C.B., Kagan, C.R. and Bawendi, M.G. (2000) Synthesis and Characterization of Monodisperse Nanocrystals and Close-Packed Nanocrystal Assemblies. *Annual Review of Materials Science*, **30**, 545-610. https://doi.org/10.1146/annurev.matsci.30.1.545

[3] Burda, C., Chen, X., Narayanan, R. and El-Sayed, M.A. (2005) Chemistry and Properties of Nanocrystals of Different Shapes. *Chemical Reviews*, **105**, 1025-1102. https://doi.org/10.1021/cr030063a

[4] Brus, L.E. (1984) Electron-Electron and Electron-Hole Interactions in Small Semiconductor Crystallites: The Size Dependence of the Lowest Excited Electronic State. *The Journal of Chemical Physics*, **80**, 4403-4409. https://doi.org/10.1063/1.447218

[5] Klimov, V.I. (2000) Optical Nonlinearities and Ultrafast Carrier Dynamics in Semiconductor Nanocrystals. *The Journal of Physical Chemistry B*, **104**, 6112-6123. https://doi.org/10.1021/jp9944132

[6] Talapin, D.V., Lee, J.S., Kovalenko, M.V. and Shevchenko, E.V. (2010) Prospects of Colloidal Nanocrystals for Electronic and Optoelectronic Applications. *Chemical Reviews*, **110**, 389-458. https://doi.org/10.1021/cr900137k

[7] Xia, Y., Yang, P., Sun, Y., Wu, Y., Mayers, B., Gates, B., *et al.* (2003) One-Dimensional Nanostructures: Synthesis, Characterization, and Applications. *Advanced Materials*, **15**, 353-389. https://doi.org/10.1002/adma.200390087

[8] Zhang, Q., Huang, J.Q., Qian, W.Z., Zhang, Y.Y. and Wei, F. (2013) The Road for Nanomaterials Industry: A Review of Carbon Nanotube Production, Post-Treatment, and Bulk Applications for Composites and Energy Storage. *Small*, **9**, 1237-1265. https://doi.org/10.1002/smll.201203252

[9] Wang, Z.L. (2006) Piezoelectric Nanogenerators Based on Zinc Oxide Nanowire Arrays. *Science*, **312**, 242-246. https://doi.org/10.1126/science.1124005

[10] Lines, M.E. and Glass, A.M. (1977) Principles and Applications of Ferroelectrics and Related Materials. Oxford University Press.

[11] Varga, T., Droubay, T.C., Bowden, M.E., Nachimuthu, P., *et al.* (2009) Coexistence of Weak Ferromagnetism and Ferroelectricity in the High Pressure $LiNbO_3$-Type Phase of $FeTiO_3$. *Physical Review Letters*, **103**, Article 047601.

[12] Shaltaf, R., Durgun, E., Raty, J.Y., Ghosez, P. and Gonze, X. (2008) Dynamical, Dielectric, and Elastic Properties of Gete Investigated with First-Principles Density Functional Theory. *Physical Review B*, **78**, Article 205203. https://doi.org/10.1103/physrevb.78.205203

[13] Lovinger, A.J. (1983) Ferroelectric Polymers. *Science*, **220**, 1115-1121. https://doi.org/10.1126/science.220.4602.1115

[14] Furukawa, T. (1989) Ferroelectric Properties of Vinylidene Fluoride Copolymers. *Phase Transitions*, **18**, 143-211. https://doi.org/10.1080/01411598908206863

[15] Martins, P., Lopes, A.C. and Lanceros-Mendez, S. (2014) Electroactive Phases of Poly (Vinylidene Fluoride): Determination, Processing and Applications. *Progress in Polymer Science*, **39**, 683-706. https://doi.org/10.1016/j.progpolymsci.2013.07.006

[16] Mendes, S.F., Costa, C.M., Caparros, C., Sencadas, V. and Lanceros-Méndez, S. (2012) Effect of Filler Size and Concentration on the Structure and Properties of Poly (Vinylidene fluoride)/$BaTiO_3$ Nanocomposites. *Journal of Materials Science*, **47**, 1378-1388. https://doi.org/10.1007/s10853-011-5916-7

[17] Yang, C., Song, H., Liu, D. and Wang, Z. (2018) Enhanced Dielectric and Ferroelectric Properties of Poly (Vinylidene Fluoride) Composites with Graphene Oxide Wrapped $BaTiO_3$ Nanorods. *Composites Science and Technology*, **159**, 67-74.

[18] Pramanik, S., Sahoo, M. and Swain, S.K. (2020) Polymer Nanocomposites for Energy Storage Applications: A Review. *Journal of Energy Storage*, **32**, Article 101829.

[19] Dang, Z.M., Yuan, J.K., Zha, J.W., Zhou, T., Li, S.T. and Hu, G.H. (2012) Fundamentals, Processes and Applications of High-Permittivity Polymer-Matrix Composites. *Progress in Materials Science*, **57**, 660-723. https://doi.org/10.1016/j.pmatsci.2011.08.001

[20] Wang, Q. and Zhu, L. (2011) Polymer Nanocomposites for Electrical Energy Storage. *Journal of Polymer Science Part B: Polymer Physics*, **49**, 1421-1429. https://doi.org/10.1002/polb.22337

[21] Tauc, J., Grigorovici, R. and Vancu, A. (1966) Optical Properties and Electronic Structure of Amorphous Germanium. *Physica Status Solidi*, **15**, 627-637. https://doi.org/10.1002/pssb.19660150224

[22] Pankove, J.I. (1971) Optical Processes in Semiconductors. Dover Publications.

[23] Mott, N.F. and Davis, E.A. (1979) Electronic Processes in Non-Crystalline Materials. 2nd Edition, Oxford University Press.

[24] Fox, M. (2010) Optical Properties of Solids. 2nd Edition, Oxford University Press.

[25] Yu, P.Y. and Cardona, M. (2010) Fundamentals of Semiconductors: Physics and Materials Properties. 4th Edition, Springer.